Mechanism of Fiber Formation by Interfacial Polyelectrolyte Complexation

Andrew C. A. Wan, I-Chien Liao, Evelyn K. F. Yim, and Kam W. Leong*

Department of Biomedical Engineering, Johns Hopkins University School of Medicine, 720 Rutland Avenue, 729 Ross Research Building, Baltimore, Maryland 21205

Received January 14, 2004; Revised Manuscript Received June 14, 2004

ABSTRACT: A four-step mechanism is hypothesized for the process of fiber formation by interfacial polyelectrolyte complexation: (1) formation of a polyionic complex film at the interface that acts as a viscous barrier to free mixing; (2) scattering of this complex by a drawing motion, creating submicron "nuclear fibers"; (3) growth of "nuclear fibers", with an accompanying decrease in the viscosity of the surrounding polyelectrolyte matrix; (4) coalescence of "nuclear fibers", resulting in a thicker primary fiber and gel droplets at regular intervals along its axis. Presented evidence include light and confocal microscopy of the fiber structure, detailed observation of the fiber drawing process, turbidity experiments to measure the stability of the interface, effect of polyelectrolyte solution concentrations and contact area at the interface on fiber dimensions, and identification of two critical draw rates that can be related to the proposed fiber-forming mechanism.

Introduction

Interface phenomena of polyelectrolyte complexes have gathered much interest in recent years. Polyelectrolyte multilayers, which are formed by the sequential layering of oppositely charged polyelectrolytes[1] have found applications in a multitude of applications, such as drug delivery devices, light emitting diodes, and antireflection coatings.[2−7] The use of these complexes to form structured materials at the micro or nanoscale levels can be extended to fiber forms. Yamamoto and co-workers have demonstrated that polyionic fibers could be drawn using combinations of polyelectrolytes such as poly(lysine)−gellan, chitosan−gellan, and chitosan−poly(acrylic acid), in a manner that suggests a self-assembly phenomenon at the polyelectrolyte solution interface.[8−13] Using the polyelectrolyte combination of water-soluble chitin and alginate, we have investigated this fiber type for biomedical application.[14] The fiber process, being aqueous-based and taking place under ambient conditions, enables the encapsulation of proteins and cells. This alleviates the use of denaturing solvents and high temperatures in conventional fiber fabrication that would be detrimental to biological materials. In this paper, we propose a basic mechanism for fiber formation by interfacial polyelectrolyte complexation (IPC), based on experimental evidence. This mechanism was clarified by investigating the effect of various parameters on the formation of fibers comprising alginate and/or heparin as the polyanions and chitosan as the polycation.

Materials and Methods

Chitosan (high molecular weight, degree of deacetylation: 75−85%, Aldrich), sodium alginate (low molecular weight, Sigma), and heparin, (cell culture grade, from porcine intestinal mucosa, Sigma) were employed. A 1% chitosan solution in 1% acetic acid possessed a viscosity of 20−200 cps, and a 2% sodium alginate solution possessed a viscosity of approximately 250 cps at 25° C. Unless stated otherwise, chitosan solutions were prepared in 0.15 M acetic acid and alginate solutions were prepared in deionized water.

Fiber Fabrication. Fiber was fabricated by drawing up the interface between two oppositely charged polyelectrolyte solutions using a bent syringe needle (25G3/8) attached to the slider of a linear motor (LinMot, Switzerland) with a stroke length of 30 cm. A LinMot Talk software allowed drawing to be performed according to pre-programmed motion profiles. The solution interface was created by first placing droplets of the polyelectrolyte solutions 1−2 mm apart on the surface of a polystyrene or Teflon plate. Droplet volumes were commonly in the range of 1−10 μL. The bent needle was used to bring the two droplets in contact and the upward drawing motion was instantly commenced.

For the measurement of critical draw rates, another configuration was employed where a droplet of alginate solution was placed above a droplet of chitosan in 0.15 M acetic acid at a volume ratio of 1:2.5, respectively. A syringe needle attached to the LinMot slider was inserted to touch the plate surface and gently aspirated to consume a small volume of the lower polyelectrolyte. The slider motion was then commenced at different draw rates. The alginate concentration was kept at 1% while the chitosan concentration was varied.

Quantum Dot Labeling of Alginate. Biotinylated alginate was prepared in the following way: 2.5 mg of sodium alginate was dissolved in 0.5 mL of 0.1 M MES buffer, pH 5.5. 104.8 μL of a solution of 36 mg/mL Biotin-XX-hydrazide (Calbiochem) in dimethyl sulfoxide was added to the alginate solution and vortexed briefly to mix. Then 12.5 μL of a 0.12 mg/μL solution of freshly prepared 1-ethyl-3-(3-(dimethylamino)propyl)carbodiimide (Sigma) solution in 0.1 M MES buffer, pH 5.5, was added to the first solution containing alginate and Biotin-XX-hydrazide. The reaction mixture was incubated for at least 2 h at room temperature. The biotinylated alginate was purified using a dialysis membrane with a molecular weight cutoff of 3500 kDa (Pierce). The molar ratio of biotin to alginate was determined using the HABA assay (Pierce), yielding a value of one biotin to every 14 alginate repeating units.

One microliter of Qdot 605 Streptavidin conjugate, 2 μM in 50 mM borate, pH 8.3 (Quantum Dot Corporation, Hayward CA), was added to 10 μL of 1% biotinylated alginate solution in deionized water. The Qdot and alginate solutions were mixed by vortexing and incubated for 10 min before drawing

* To whom correspondence should be addressed. E-mail addresses for all authors: A.C.A.W., awan@bme.jhu.edu; I-C.L., icliao@bme.jhu.edu; E.K.F.Y., eyim@bme.jhu.edu; K.W.L., kleong@bme.jhu.edu.

10.1021/ma0498868 CCC: $27.50
Published on Web 08/06/2004

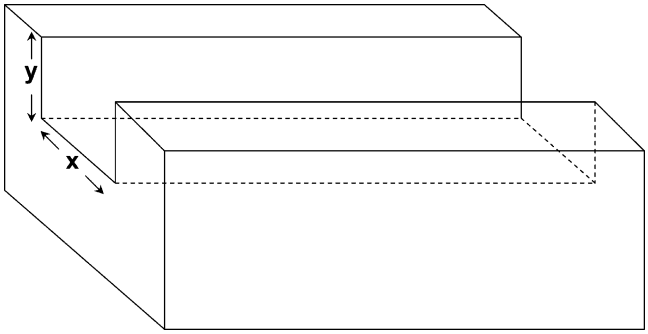

Figure 1. Channels were carved into Teflon blocks to define the cross sectional area of contact between the polyelectrolyte solutions. One channel is depicted in the illustration, the dotted lines delimit the inner surface of the channel. The cross-sectional area of the channel = ($x \times y$).

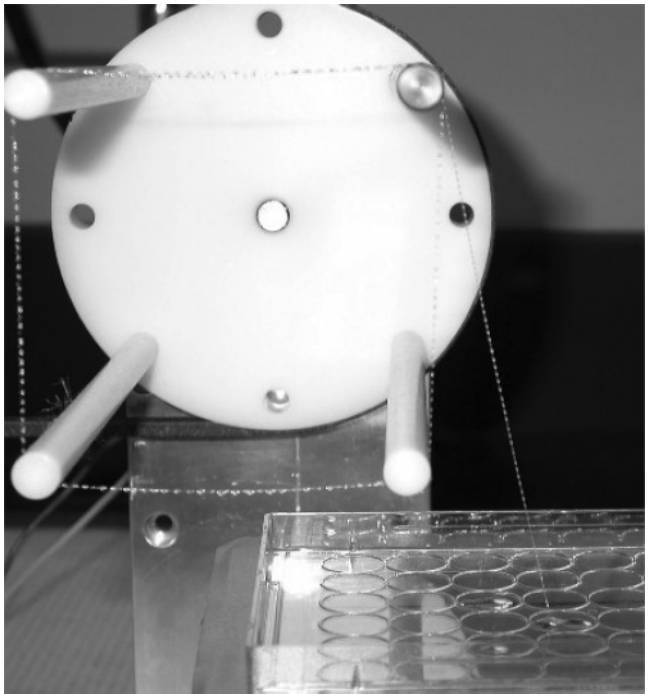

Figure 2. Process of fiber formation by interfacial polyelectrolyte complexation. Continuous fiber production can be achieved by means of a roll-up apparatus.

fiber. Fibers were drawn using 5 μL each of the labeled alginate and 1% chitosan solutions. The fiber was examined under the confocal microscope, employing excitation/emission wavelengths of 530 nm/605 nm.

Effect of Interfacial Area and Polyelectrolyte Concentration on Fiber Dimensions. The interfacial area of contact between the two polyelectrolyte solutions was defined by using channels of varying cross-sectional areas, which were carved into Teflon blocks (Figure 1). Droplets of the two polyelectrolyte solutions of equal volume were transferred into these channels and placed adjacent to each other. A pair of forceps was used to pinch the region of the interface and fiber was drawn, then adhered to the roll-up apparatus (Figure 2), revolving at a rate of 2.5 revolutions/min. The chitosan and alginate concentrations were maintained at 1% (w/v) and 0.5% (w/v), respectively. The influence of alginate and chitosan solution concentrations on fiber dimensions was investigated by drawing fiber from an interfacial area of 3 mm^2.

Effect of Viscosity on the Stability of the Interface. First 100 μL samples of various concentrations of chitosan solution were added to a 96-well plate, and 50 μL of alginate or heparin solution was carefully introduced into each of the heparin-containing wells, via the side of the well. The 96-well plate was placed into a microplate reader (Bio-Rad, model 550) and measurement of the absorbance at 450 nm was immediately commenced, at 30 s sampling intervals. The turbidity profile for each sample was obtained in terms of absorbance vs time. Three samples were measured for each concentration pair to obtain statistical significance.

Images of Fiber Drawing (Light Microscope). Ten microliters of 0.125% chitosan solution was placed approximately 2 mm from 10 μL of 1% alginate solution on a glass slide staged on an optical microscope. Using a pair of forceps, the solutions were brought together and fiber was produced by pulling the forceps upward, away from the solution. A camera was mounted onto the light microscope to capture the images of fiber being drawn from the solution interface, at a magnification of 100×.

Silica Gel Encapsulation. Chitosan with a degree of deacetylation of 54% was prepared by the partial deacetylation of chitin[15] (practical grade, Sigma). Silica gel (Aldrich, mean particle diameter of 6 μm, 70−230 mesh) was dispersed in alginate solution and fiber was drawn at a draw rate of 20 mm/s using the linear motor (LinMot).

Results and Discussion

Fiber can be drawn by placing droplets of two oppositely charged polyelectrolyte solutions in close proximity on a level surface, bringing them in contact, then drawing upward by means of a forceps or bent needle. Fiber can be drawn from the interface until one of the polyelectrolyte phases is depleted, and continuous fiber formation can be achieved by means of a roll-up apparatus (Figure 2). The process of fiber drawing by interfacial polyelectrolyte complexation is reminiscent of the "nylon rope trick" which illustrates the interfacial polycondensation of polyamides.[16] However, a completely different mechanism of fiber formation is involved in interfacial polyelectrolyte complexation, as the present study shows. Unlike interfacial polycondensation, which is essentially a polymerization reaction, interfacial polyelectrolyte complexation is driven by the insolubilization of oppositely charged polyelectrolytes as a result of the neutralization of charges.

At a glance, the most striking feature of fibers formed via the process of interfacial polyelectrolyte complexation is its unusual morphology of a "primary fiber", with beads spaced out at regular intervals along the fiber axis. These beads take the form of viscous fluid droplets when freshly drawn, which become protuberances upon drying (Figure 3A). The surface of the primary fiber is composed of parallel ridges and valleys, as if it were composed of a conglomerate of finer fibers (Figure 3B). This "venation" pattern has also been noted by other workers.[12] We could show that the fiber was indeed made up from a collection of thinner fibers. When nascent fiber was drawn and immediately placed in contact with a glass slide, the gel droplets spread out into two-dimensional beadlike structures. Within these regions, the primary fiber could be seen to fan out into individual fibers of submicron diameter, resulting in an onionlike venation pattern (Figure 3C). When quantum dot labeled alginate was used to draw fiber with chitosan, which was air-dried and visualized using confocal microscopy, regions of fluorescence corresponding to these thinner fibers were observed (Figure 3D). In the dry form, most of these thinner fibers were observed to traverse the longitudinal axis of the primary fiber. In the bead region, the fluorescence was localized to the fibers and not the surrounding matrix, implying a much higher density of polyelectrolyte complex in the fiber, compared to the matrix. (Both fiber and matrix are constituted of a polyelectrolyte complex, deduced by

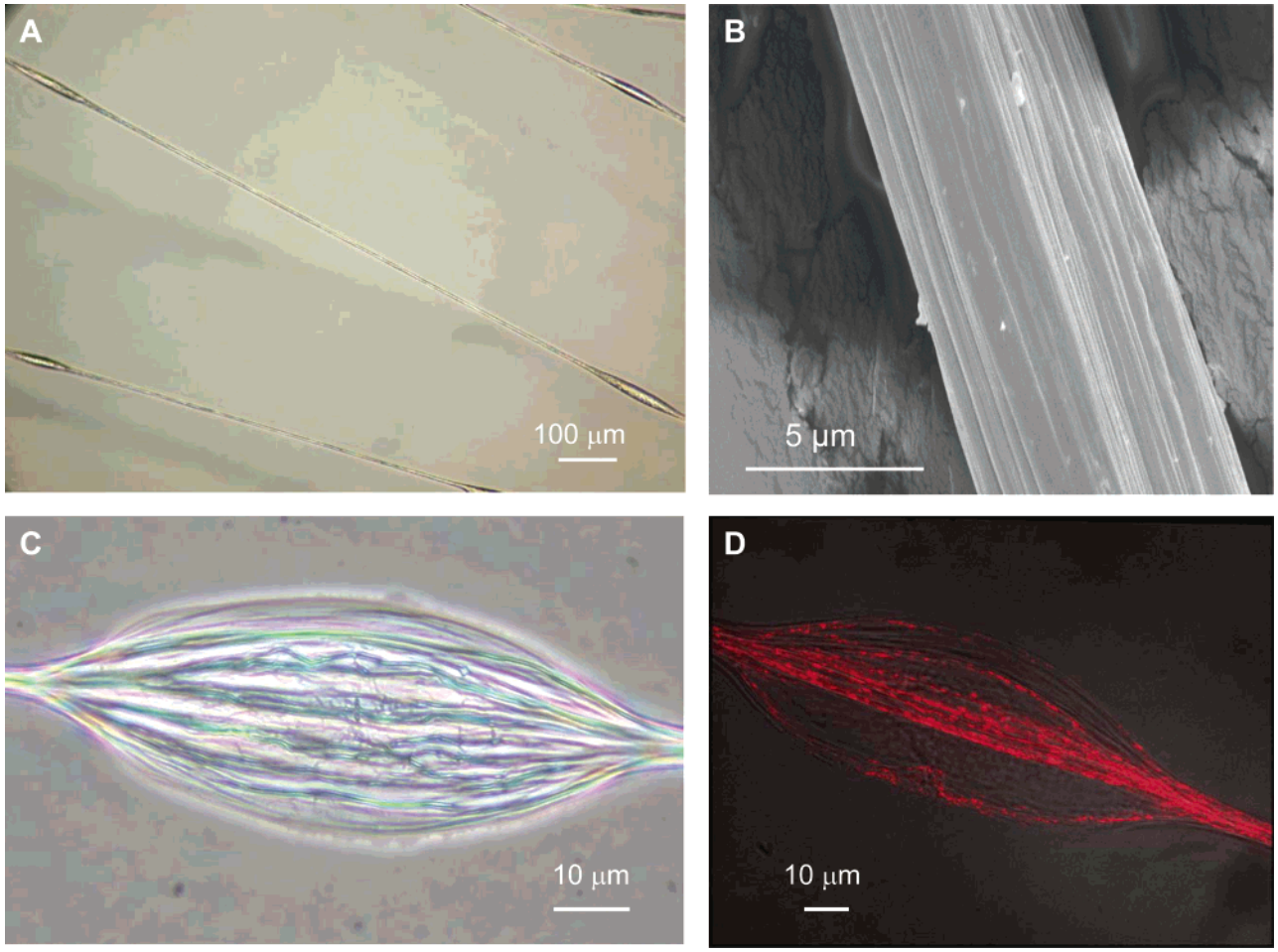

Figure 3. (A) Light microscope image of several air-dried fiber strands. (B) Fiber surface, composed of parallel ridges. (C) Individual "nuclear" fibers spread out in the bead region of a nascent fiber that was immediately adhered upon a glass slide. (Scale bar = 10 μm.) (D) Confocal micrograph of fiber composed of water soluble chitin and alginate labeled with quantum dots.

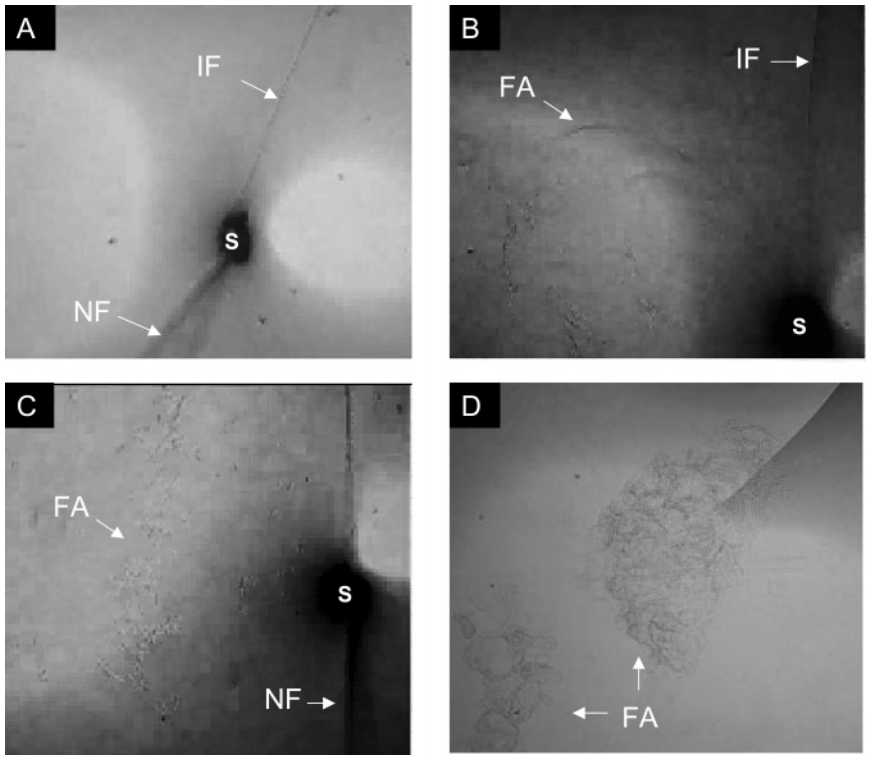

Figure 4. Light microscope stills of the fiber drawing process: NF, nascent fiber; S, source; FA, fibrillar aggregate; IF, interface.

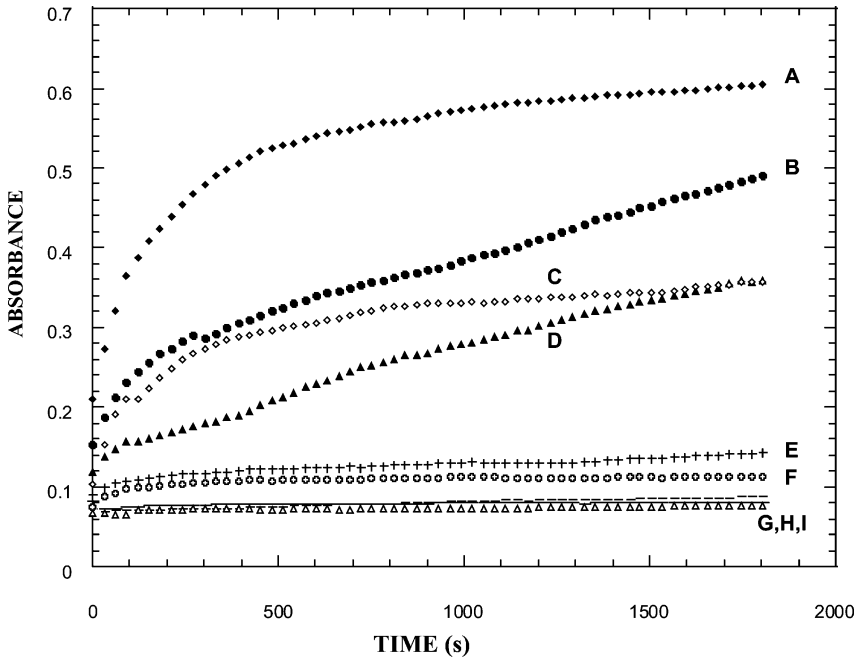

Figure 5. Turbidity curves from the contact of chitosan and alginate solutions; (chitosan, alginate concentrations in % w/v): + (0.125, 0.5); - - (0.25, 0.5); − (0.5, 0.5); ◆ (0.125, 0.125); ● (0.25, 0.125); ▲ (0.5, 0.125); ◇ (0.125, 0.25); ○ (0.25, 0.25); △ (0.5, 0.25).

Table 1. Stability of the Interface between Chitosan and Alginate Solutions of Various Concentrations, As Indicated by the Development or Absence of Turbidity[a]

		heparin concentration (% w/v)			
		0.5	1.0	1.5	2.0
chitosan concentration (% w/v)	0.125	●	●	●	●
	0.25	●	●	●	●
	0.3	●	●	○	○
	0.4	●	○	○	○
	0.5	○	○	○	○
	0.6	○	○	○	○

[a] Key: (●) turbid (unstable); (○) clear (stable).

Table 2. Stability of the Interface between Chitosan and Heparin Solutions of Various Concentrations, As Indicated by the Development or Absence of Turbidity[a]

		alginate concentration (% w/v)			
		0.125	0.25	0.5	1.0
chitosan concentration (% w/v)	0.125	●	●	●	○
	0.25	●	●	○	○
	0.3	●	○	○	○
	0.4	●	○	○	○
	0.5	●	○	○	○
	0.6	●	○	○	○

[a] Key: (●) turbid (unstable); (○) clear (stable).

the fact that they are water insoluble even when their original polyelectrolyte solutions are water-soluble.)

As a first step to understand how these finer fibers formed in the IPC process, we used light microscopy to probe the details of the fiber formation process. First, it was clearly seen that a defined interface was always present during fiber drawing (Figure 4A), and the nascent fiber emerged from this interface. It could be reasonably deduced that complex was being formed and drawn up in the form of fiber, while fresh polyelectrolyte continuously diffused toward and replenished the interface. Additionally, it was also observed that a fibrillar aggregate or precipitate was continuously being formed, which radiated outward from the fiber-solution junction, and which was not incorporated into the fiber (Figure 4B,C). These aggregates eventually disrupted the interface, leading to fiber termination (Figure 4D).

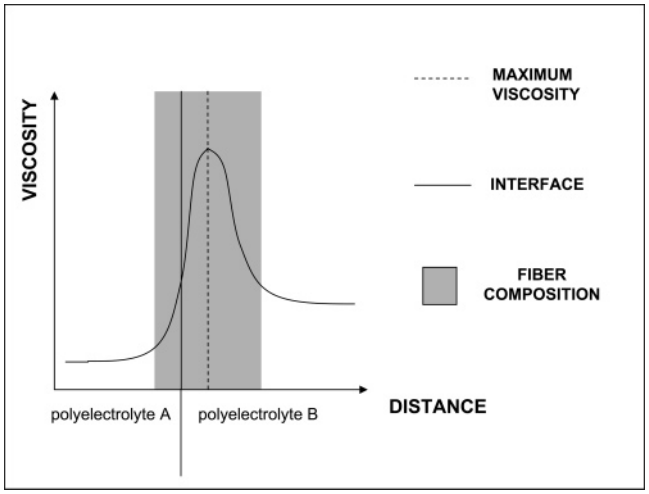

Figure 6. Diagrammatic representation of the interface between two polyelectrolyte solutions.

A viscous barrier at the junction between the two polyelectrolytes, apparent in the form of a defined interface, was deemed important for the formation of fiber by the IPC process. In our experiments with different combinations of polyelectrolytes, it appeared that a requisite charge density was essential for fiber formation. Oppositely charged polyectrolytes with lower charge densities did not form a distinct interface region at any concentration, and gradually formed a complex precipitate when mixed. Polyelectrolytes that did form fiber required minimum concentrations in order to form fiber continuously. At low concentrations, fiber could form, but terminated before all of the polyelectrolyte solution could be depleted, concomitant with the development of a precipitate in the solution.

These observations suggested that the ability to draw fiber continuously was related to a balance between the stability of the interface and the precipitation of a polyionic complex in the solution. To investigate this

Table 3. Dependence of Fiber Dimensions on the Interfacial Area between Two Polyelectrolyte Solutions

area of interface (mm^2)	0.5	1	3	4	5
[channel width (mm) × depth (mm)]	[1 × 0.5]	[1 × 1]	[3 × 1]	[4 × 1]	[5 × 1]
fiber diameter (μm)	1.14 ± 0.34[a]	1.44 ± 0.47	2.20 ± 0.10	2.50 ± 0.25	2.32 ± 0.33
bead diameter (μm)	7.00 ± 0.54	11.93 ± 1.16	24.80 ± 0.89	30.50 ± 2.73	29.52 ± 4.21

[a]Mean ± standard deviation.

Table 4. Dependence of Fiber Dimensions on the Alginate Solution Concentration

alginate concentration (% w/v)	0.5	0.75	1	1.25	1.5
fiber diameter (μm)	1.28 ± 0.35[a]	1.86 ± 0.44	2.20 ± 0.10	2.19 ± 0.25	2.20 ± 0.32
bead diameter (μm)	6.59 ± 4.47	14.49 ± 1.33	24.80 ± 0.89	21.30 ± 2.24	21.40 ± 2.89

[a]Mean ± standard deviation.

Table 5. Dependence of Fiber Dimensions on the Chitosan Solution Concentration

chitosan concentration (% w/v)	0.125	0.25	0.5	0.75
fiber diameter (μm)	2.13 ± 0.07[a]	2.30 ± 0.29	2.20 ± 0.10	2.06 ± 0.20
bead diameter (μm)	10.75 ± 0.66	15.72 ± 1.27	24.80 ± 0.89	27.19 ± 0.45

[a]Mean ± standard deviation.

further, we performed turbidimetric experiments where polyelectrolyte pairs of different concentrations were placed, one above the other in microwell plates. The formation of precipitate, if any, was monitored by the decrease in intensity of light passing through the solutions; precipitation was accompanied by opacity that resulted in a measured absorbance. Figure 5 illustrates the set of curves that was obtained for combinations of chitosan and alginate concentrations ranging between 0.125 and 0.5% (w/v). Rapid development of turbidity was observed for the lower concentration pairs (curves A−D). In general, the rate of precipitation was faster at the beginning, and gradually tapered with time. As the concentrations of the polyelectrolytes were increased, the rate of precipitation and quantity of precipitate formed were decreased (curves E and F). For the highest concentrations used, there was no precipitation at all within the time frame of the experiment (curves G−I). For these concentration pairs, the interface was considered to be stable.

The results in terms of interfacial stability are summarized in Tables 1 and 2 for the two polyelectrolyte pairs, chitosan-alginate and chitosan-heparin. The ability of the polyelectrolyte pairs to remain in contact indefinitely without developing any turbidity was a function of both, and not just one, of the polyelectrolyte concentrations. This showed that the formation of a barrier toward free mixing of the polyelectrolytes was due to an interaction between the two components, presumably in the form of a complex film at the interface. This complex film would be similar in nature to the flat interfaces formed by polyelectrolyte layers, which exhibit selective permeability.[17] As compared to alginate, heparin required higher solution concentrations in order to maintain a stable interface with the chitosan solution. This was due to the lower molecular weight of heparin (<30 kDa) compared to chitosan (≈300 000 kDa) used in the experiment, thus needing higher concentrations to achieve the requisite viscosity.

A diagrammatic representation of the interface region, plotted in terms of viscosity vs distance from the interface, is shown in Figure 6. Ionic complexation of the two polyelectrolytes at, or near the interface results in an increase in the viscosity. This viscous barrier prevents free mixing of the two polyelectrolytes, thus preventing precipitation from occurring. The nascent complex that is removed from this interface by an upward motion can be imagined to form a fiber centered

Table 6. Ability to Draw Fiber, and Type of Fiber Formed at Various Draw Rates and Concentrations of Chitosan Solution[a]

		Drawing rate (mm/s)									
		0.25	0.5	1	2	5	10	20	30	40	60
Chitosan concentration (%w/v)	0.125										
	0.25										
	0.50										
	0.75										

[a] Sodium alginate was used as the polyanion. Shaded region indicates the draw rates at which fiber could be drawn successfully; in the darker region, a beadless fiber was drawn.

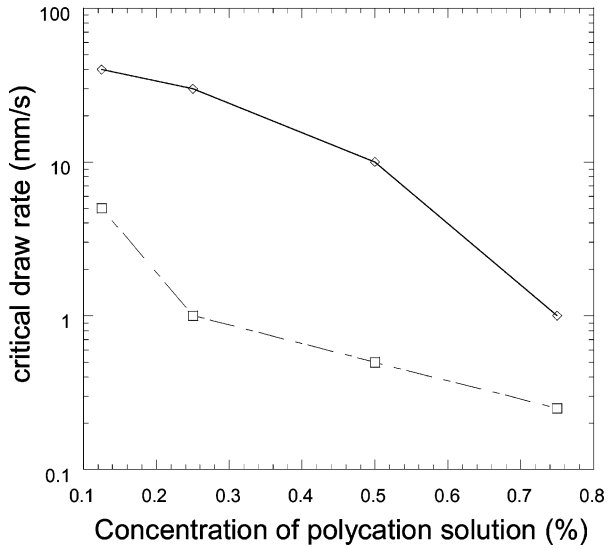

Figure 7. Dependence of critical draw rates on the concentration of chitosan in 0.15 M acetic acid: (◇) fiber point; (□) bead point.

upon the region of maximum viscosity (shaded area). At lower interfacial areas, the dimensions of the fibers were directly related to the area of contact between the two polyelectrolytes, reflecting the interfacial nature of the process. At and above an interfacial area of 3 mm^2 however, a plateau was observed for both bead and fiber diameters. Fiber dimensions were also proportional to polyelectrolyte solution concentrations at lower concentrations and leveled off at higher concentrations. (Tables 4 and 5).

What happens when this viscous polyelectrolyte complex is drawn upward in a steady nascent stream? Simple observation revealed that, within a few seconds,

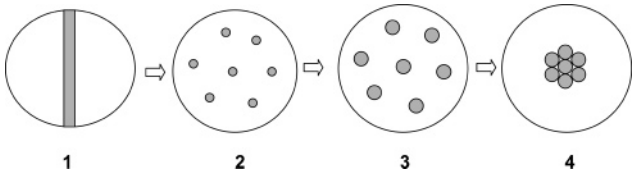

Figure 8. Steps in the hypothesized mechanism of fiber formation by interfacial polyelectrolyte complexation (fiber cross-sectional area): (1) creation of a polyionic complex film at the junction between two polyelectrolyte solutions; (2) disruption of the interface by the drawing process leads to scattered domains of complexation that act as fiber nucleation sites; (3) growth of "nuclear" fibers, accompanied by decrease in viscosity of surrounding matrix; (4) coalescence of "nuclear" fibers, leading to the formation of gel droplets (beads) along the fiber axis.

this nascent stream had collapsed into a strand of fiber and its associated droplets. The rate of droplet formation appeared to be inversely proportional to the viscosity of the polyelectrolyte solutions that were used. This bead formation occurred very rapidly (within 1−2 s), and any attempt to measure the formation time directly would have been severely inaccurate. Fortunately, another method was found to quantify the bead formation phenomenon.

Depending on the draw rate, two types of fiber could be formed, "beaded" fiber or "beadless" fiber (Table 6). "Beadless" fiber was formed at low draw rates, due to the coalescence of droplets at the solution−air interface; i.e., the draw rate was slow enough that the droplets had formed before they could leave the solution. The critical draw rate at which beadless fiber formed was defined as the "bead point". From Table 6, it can be observed that the "bead point" was inversely proportional to the concentration of chitosan solution that was used to draw fiber. In other words, this showed that beads formed more slowly for the more viscous solutions, pointing to a diffusion-dependent mechanism for bead formation.

In addition to the "bead point", a second critical draw rate could also be identified. This was the draw rate above which no fiber could be drawn, and was termed the "fiber point". The more viscous the solution, the slower the draw rate required in order to draw fiber successfully (Table 6). Thus, the "fiber point" corresponds to the initial fiber formation event that gives structural integrity to the fiber form. Similarly to bead formation, this process occurred more slowly in more viscous solutions, and was also likely to be diffusion-dependent.

Both critical draw rates were plotted together on the same axes (Figure 7). The very fact that two critical draw rates can be observed indicates that the fiber formation is constituted of two separate diffusion-dependent phenomena: an initial fiber formation, followed by a second event that results in bead formation.

Mechanism of Fiber Formation. From the experiments and data that have been described, a hypothesis for the mechanism of fiber formation is presented, with reference to Figure 8. The process can be divided into four stages.

I. Formation of Viscous Barrier at the Interface. The reactants in interfacial polyelectrolyte complexation are both dissolved in an aqueous phase. In order that the complexation remains an interfacial phenomenon, free mixing between the two phases must be avoided. This condition is satisfied by the formation of a polyelectrolyte complex "film" at the interface that acts as a viscous barrier to limit exchange of the polyelectrolytes.

II. Nucleation. As the fiber is drawn, the interface is broken down into many individual, complexed domains. These complexed regions are now freed from their kinetic constraint due to mixing with fresh polyelectrolytes and act as nucleation sites for further complexation. This occurs very rapidly (polyelectrolyte complex formation has been shown to take place in less than 5 μs[18]) to form individual "nuclear" fibers.

III. Growth of "nuclear fibers". As these "nuclear" fibers increase in size, the viscosity of the free excess component outside the fibers decreases, due to a decrease in its concentration and an increase in the ionic strength of the medium, which results from the release of salt counterions.[19]

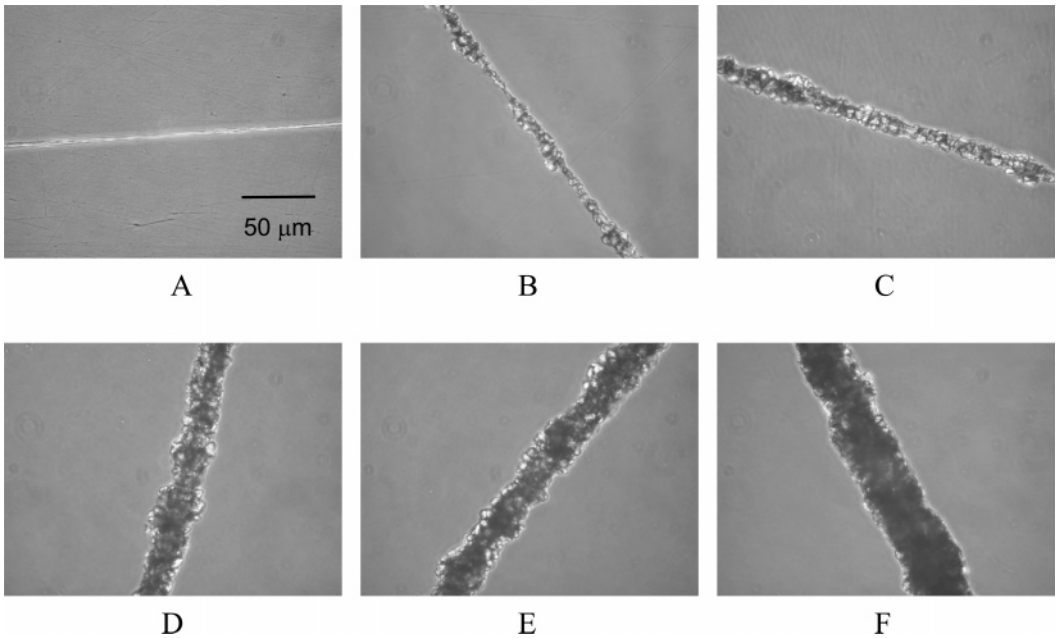

Figure 9. Light microscope images of silica gel encapsulated in chitosan-alginate fibers; Silica gel was dispersed in alginate solution at concentrations of (A) 0, (B) 10, (C) 30, (D) 50, (E) 100, and (F) 150 mg/mL. All photos are at the same magnification.

IV. Coalescence of "Nuclear Fibers". These "nuclear" fibers eventually coalesce, and the excess polyelectrolytes form gel droplets along the fiber axis. Coalescence of the polyelectrolyte complex fibers would require either a zero-net charge or complete screening of the net-charge by the salt counterions.

As "nuclear fiber" formation and growth and "nuclear fiber" coalescence are diffusion-controlled and expected to be inversely proportional to solution viscosity, this allows us to relate "nuclear" fiber formation/growth to the "fiber point" and their coalescence to the "bead point" respectively.

Encapsulation of Materials. The IPC fiber process is unique in its ability to encapsulate materials at ambient temperature and under aqueous conditions, a feature which is especially useful for the encapsulation of biologics. The mode of IPC fiber formation which is hypothesized to involve thin "nuclear" fibers that coalesce provides a mechanism by which particulate materials can be encapsulated within the fiber without unduly compromising its physical properties, enabling the fiber to go "around" the particles. In other fiber types, any trapped particles would effectively reduce the fiber cross section and reduce its mechanical strength, if not terminating it completely.

For the encapsulation experiments, a water-soluble chitosan of degree of deacetylation approximately 50% was used, as it could be dissolved in pure water. In contrast, dissolution of chitosan with higher degrees of deacetylation requires low pHs, which may be deleterious to some of types of encapsulants, for example, cells. The encapsulation feature of the fiber process was illustrated using silica gel. Encapsulation was performed by dispersing silica gel in alginate solution, then drawing fiber against a purely aqueous chitosan solution. Figure 9 shows the appearance of silica gel encapsulated within the fiber obtained using different concentrations of the silica gel suspension in alginate. As the silica gel concentration (w/v alginate solution) was increased, a thicker fiber diameter resulted, with an accompanying increase in the quantity of dispersed phase per unit length of fiber. A greater than 10-fold increase in fiber diameter resulted when silica gel was encapsulated at a particle density of 150 mg/mL of alginate solution. Dispersion of silica gel in alginate solution increases its viscosity in proportion to the concentration, and broadens the viscous region of the interface depicted in Figure 6. This produces an effect similar to increasing the concentration of alginate, leading to a thicker fiber.

In summary, a hypothesis for the mechanism of fiber formation by interfacial polyelectrolyte complexation is presented based on experimental evidence. Increasing interest in this fiber type and process is expected in the near future, not only for the novelty of the fiber formation phenomenon, but for its potential application in areas of therapeutic engineering and regenerative medicine.

Acknowledgment. A.C.A.W. wishes to acknowledge The Agency for Science, Technology and Research, Singapore (A-STAR) for a National Science Scholarship. We thank S.H. Lim and J. Wang for helpful discussions.

References and Notes

(1) Decher, G. *Science* **1997**, *277*, 1232.
(2) Hammond, P. *Curr. Opin. Colloid Interface Sci.* **1999**, *4*, 430.
(3) Thierry, B.; Winnik, F.; Merhi, Y.; Silver, J.; Tabrizian, M. *Biomacromolecules* **2003**, *4*, 1564.
(4) Ai, H.; Jones, S.; Lvov, Y. *Cell Biochem. Biophys.* **2003**, *39*, 23.
(5) Hiller, J.; Mendelsohn, J.; F, R. *Nat. Mater.* **2002**, *1*, 59.
(6) Hong, H. *Supramol. Sci.* **1997**, *4*, 67.
(7) Ibarz, G.; Dahne, L.; Donath, E.; Mohwald, H. *Adv. Mater.* **2001**, *13*, 1324.
(8) Ohkawa, K.; Ando, M.; Shirakabe, Y.; Takahashi, Y.; Yamada, M.; Shirai, H.; Yamamoto, H. *Text. Res. J.* **2002**, *72*, 120.
(9) Ohkawa, K.; Takahashi, Y.; Yamamoto, H. *Macromol. Rapid Commun.* **2000**, *21*, 223.
(10) Ohkawa, K.; Shoumura, K.; Shirakabe, Y.; Yamamoto, H. *J. Mater. Sci.* **2003**, *38*, 3191.
(11) Yamamoto, H.; Senoo, Y. *Macromol. Chem. Phys.* **2000**, *201*, 84.
(12) Yamamoto, H.; Horita, C.; Senoo, Y.; Nishida, A.; Ohkawa, K. *J. Appl. Polym. Sci.* **2001**, *79*, 437.
(13) Hachisu, M.; Ohkawa, K.; Yamamoto, H. *Macromol. Biosci.* **2003**, *3*, 92.
(14) Wan, A.; Yim, E.; Liao, I.; LeVisage, C.; Leong, K. *J. Biomed. Mater. Res.* **2004**, in press.
(15) Sannan, T.; Kurita, K.; Iwakura, Y. *Makromol. Chem.* **1976**, *177*, 3589.
(16) Morgan PW, K. S. *J. Polym. Sci., Part A: Polym. Chem.* **1996**, *34*.
(17) Schwarz, H.-H.; Lukas, J.; Richau, K. *J. Membr. Sci.* **2003**, *218*, 1.
(18) Bakeev, K.; Izumrudov, V.; Zezin, A. *Dokl. Akad. Nauk* **1988**, *299*, 1405.
(19) Dautzenberg, H. *Macromol. Symp.* **2000**, *162*, 1.

MA0498868